NACA

RESEARCH MEMORANDUM

SMALL-SCALE TRANSONIC INVESTIGATION OF THE EFFECTS OF TWIST AND CAMBER ON THE AERODYNAMIC CHARACTERISTICS OF A 60° 42' SWEPTBACK WING OF ASPECT RATIO 1.94

By Kenneth P. Spreemann and William J. Alford, Jr.

Langley Aeronautical Laboratory
Langley Field, Va.

NATIONAL ADVISORY COMMITTEE
FOR AERONAUTICS

WASHINGTON
January 10, 1952

NATIONAL ADVISORY COMMITTEE FOR AERONAUTICS

RESEARCH MEMORANDUM

SMALL-SCALE TRANSONIC INVESTIGATION OF THE EFFECTS OF TWIST AND CAMBER ON THE AERODYNAMIC CHARACTERISTICS OF A 60° 42' SWEPTBACK WING OF ASPECT RATIO 1.94

By Kenneth P. Spreemann and William J. Alford, Jr.

SUMMARY

A small-scale transonic investigation of two semispan wings having the same plan form was conducted in the Langley high-speed 7- by 10-foot tunnel over a Mach number range of 0.59 to 1.10 to determine the effects of twist and camber on the aerodynamic characteristics of a 60° 42' sweptback wing of aspect ratio 1.94. The semispan wings had taper ratios of 0.44 and modified NACA 64A-series airfoil sections tapered in thickness. Lift, drag, pitching moment, and root bending moment were obtained for the two wings investigated.

The results of the investigation indicate that the benefits of twist and camber for the wings with 60° 42' sweepback were considerably smaller than the benefits obtained at the design condition (uniform loading at a lift coefficient of 0.25 and Mach number of 1.10 at 50° 38' sweepback). However, no adverse effects of twist and camber were noted at the higher sweep angle.

INTRODUCTION

An investigation of the effects of twist and camber on the lift, drag, and pitching-moment characteristics of a low aspect-ratio sweptback wing is reported in reference 1. For the wing investigated, the twist and camber distributions were selected to provide uniform loading at a lift coefficient of 0.25 and a Mach number of 1.10 at 50° 38' sweepback. The aerodynamic characteristics of the wing designed in this manner were shown to be considerably better than those of a wing of the same plan form but without twist and camber. Because of current interest in wings with variable sweep, determination of the aerodynamic characteristics of the wings of reference 1 when rotated from the design sweep angle (50° 38') to a higher sweep angle was considered desirable.

The present investigation is concerned with a comparison of the aerodynamic characteristics of the twisted and cambered wing and the corresponding untwisted and uncambered wing (referred to as the flat wing) with the sweep angle of the quarter-chord lines adjusted to 60° 42'. The investigation was conducted in the Langley high-speed 7- by 10-foot tunnel over a Mach number range from 0.59 to 1.10. Lift, drag, pitching moment, and root bending moment were obtained for the wing-alone configurations.

COEFFICIENTS AND SYMBOLS

C_L lift coefficient (Twice semispan lift/qS)

C_D drag coefficient (Twice semispan drag/qS)

C_m pitching-moment coefficient referred to $0.25\bar{c}$ (Twice semispan pitching moment/$qS\bar{c}$)

C_B bending-moment coefficient about axis parallel to relative wind and in plane of symmetry $\left(\text{Root bending moment}\Big/q\,\frac{S}{2}\,\frac{b}{2}\right)$

q effective dynamic pressure over span of model, pounds per square foot $\left(\frac{1}{2}\rho V^2\right)$

S twice wing area of semispan model, 0.129 square foot

$\bar{c}$ mean aerodynamic chord of wing, 0.273 foot, based on relationship $\frac{2}{S}\int_0^{b/2} c^2 dy$ (using theoretical tip)

c local wing chord parallel to plane of symmetry, feet

b twice span of semispan model, 0.51 foot

y spanwise distance from plane of symmetry, feet

ρ air density, slugs per cubic foot

V effective stream velocity over model, feet per second

M effective Mach number $\left(\frac{2}{S}\int_0^{b/2} cM_a\, dy\right)$

[redacted]

M_l	local Mach number
M_a	average chordwise Mach number
R	Reynolds number $(\rho V\bar{c}/\mu)$
μ	absolute viscosity, pound-seconds per square foot
α	angle of attack of $\bar{c}$, degrees
ϵ	local angle of streamwise wing twist, degrees
d	chordwise distance from wing leading edge measured parallel to streamwise chord line, feet
z	camber (distance above c), feet
$y_{c.a.l.}$	lateral center of additional loading, percent semispan $\left(100\,\frac{\partial C_B}{\partial C_L}\right)$
$C_{m_{C_{L=0}}}$	pitching-moment coefficient at zero lift coefficient
$C_{D_{min}}$	minimum drag coefficient
$C_{L_{C_{D_{min}}}}$	lift coefficient at minimum drag coefficient
$(L/D)_{max}$	maximum lift-drag ratio
$C_{L_{(L/D)_{max}}}$	lift coefficient at maximum lift-drag ratio

MODELS AND APPARATUS

The steel wings of the flat and the twisted and cambered semispan models had 60° 42' of sweepback referred to their quarter-chord lines, aspect ratios of 1.94, and taper ratios of 0.44. The airfoil sections of the flat wing perpendicular to the 31.5-percent-chord line, where the 31.5-percent-chord line intersects the streamwise root and tip chords, were NACA $64_{(10)}$A011.2 at the root and NACA $64_{(08)}$A008.1 at the tip. The same 64A-series airfoil thickness distribution was placed around the mean camber surface of the twisted and cambered wing. The maximum streamwise thicknesses were 6.2 percent at the root and 4.5 percent at the tip.

[redacted]

A two-view drawing of the models is presented in figure 1. Included in this figure are pertinent geometric data of the two wings investigated. A photograph of a typical sweptback-wing model mounted on the reflection-plane setup in the Langley high-speed 7- by 10-foot tunnel is presented in figure 2.

The wings of the present investigation are the same wings of reference 1 except that the panels have been rotated backward to provide a larger sweep angle. The increased sweep angle resulted in reductions in the streamwise thickness ratio and camber. The maximum camber was moved back to about the 42.5-percent streamwise chord throughout the span as a result of increasing the sweep angle. The camber, maximum camber, and the angle of wing twist of the twisted and cambered wing of the present investigation are presented in figure 3.

Force and moment measurements were made with a strain-gage-balance system and recorded with recording potentiometers. The angle of attack was measured by means of a slide-wire potentiometer and recorded with a recording potentiometer.

TESTS

The investigation was conducted in the Langley high-speed 7- by 10-foot tunnel with the model mounted on a reflection-plane plate (fig. 1) located 3 inches from the tunnel wall in order to bypass the wall boundary layer. The reflection-plane boundary-layer thickness was such that a value of 95 percent of free-stream velocity was reached at a distance of approximately 0.16 inch from the surface of the reflection plane at the balance center line for all test Mach numbers. This boundary-layer thickness represented a distance of about 5 percent semispan for the models tested.

At Mach numbers below 0.93 there was practically no velocity gradient in the vicinity of the reflection plane. At higher Mach numbers, however, the presence of the reflection plane created a high local-velocity field which permitted testing the small models up to $M = 1.10$ before choking occurred in the tunnel. The variations of local Mach numbers in the region occupied by the models are shown in figure 4. Effective test Mach numbers were obtained from additional contour charts similar to those shown in figure 4 by the relationship $M = \frac{2}{S}\int_0^{b/2} cM_a \, dy$.

For the models tested, Mach number variations (outside of the boundary layer) of less than 0.01 over the surface of the models generally

were obtained below $M = 0.95$. Local Mach number variations of 0.05 and about 0.07 were obtained at $M = 0.98$ and $M = 1.10$, respectively. It should be noted that the Mach number variations of this investigation are principally chordwise, whereas the Mach number variations of reference 1 are principally spanwise.

A gap of about 1/16 inch was maintained between the wing-root-chord section and the reflection-plane-plate turntable and a sponge-wiper seal was fastened to the wing butt behind the turntable to minimize leakage. Force and moment measurements were made for the models over a Mach number range from 0.59 to 1.10 and an angle-of-attack range from -8° to 22°. The pitching moments were measured about the 22-percent-chord point of the mean aerodynamic chord and were transferred to the quarter-chord point of the mean aerodynamic chord. The variation of Reynolds number with Mach number for these tests is shown in figure 5.

No attempt has been made to apply corrections for jet-boundary or blockage effects. Because of the small size of the models these corrections are believed to be negligible. Corrections due to aeroelastic effects were less than 1.0 percent and were not applied to the data.

RESULTS AND DISCUSSION

The basic data of the investigation are shown in figure 6. The discussion is based principally on the summary curves presented in figure 7. Since the characteristics were rather nonlinear, the slopes presented in figure 7 were averaged over a limited lift-coefficient range of ± 0.1.

Lift Characteristics

The lift-curve slopes (fig. 7) were practically unaffected by twisting and cambering the wing. The values of $\partial C_L/\partial \alpha$ at subsonic speeds are somewhat higher than predicted by calculations based on reference 2 (see tabulated values in table I).

The angle of attack for zero lift, $\alpha_{C_{L=0}}$, was decreased about 0.2° to 0.6° throughout the Mach number range investigated by the addition of twist and camber.

The lateral center of additional loading, $y_{c.a.l.}$, for the twisted and cambered wing was no more than 1 percent outboard of that of the flat wing throughout the Mach number range investigated. The experimental

[redacted]

lateral centers of additional loading very closely approximated those predicted by theoretical calculations made by using the method of reference 2 (see values listed in table I).

Drag Characteristics

Twisting and cambering the wing caused only slight changes in the shapes of the drag curves but did shift the curves in such a manner as to cause a given drag value to occur at a higher lift coefficient. The minimum drag coefficients $C_{D_{min}}$ (fig. 7) appear to be hardly affected by twisting and cambering the wing. Similar effects were noted in the previous investigation of the wings with 50° 38' sweepback. The lift coefficients for $C_{D_{min}}$ were only slightly increased (less than 0.02) due to twisting and cambering the wing.

Lift-Drag Ratios

It can be seen in the basic data (fig. 6) that the lift-drag ratios of the twisted and cambered wing were somewhat higher than those of the flat wing except at very low lift coefficients where the lift-drag ratios were sometimes slightly higher for the flat wing. The twisted and cambered wing gave very little increase in the maximum lift-drag ratios below a Mach number of 0.95 and above a Mach number of 1.05 (fig. 7); however, in the Mach number range between 0.95 and 1.05 the twisted and cambered wing produced about 6 to 12 percent higher maximum lift-drag ratios than the untwisted, uncambered wing. Reverse effects of Mach number on $(L/D)_{max}$ were noted for the 50° 38' swept wing in reference 1, wherein the highest percentage increases in $(L/D)_{max}$ were obtained at the lowest Mach numbers investigated. The value of C_L for $(L/D)_{max}$ was slightly higher for the twisted and cambered wing above 0.85 Mach number which was the range wherein the maximum percentage increases were noted in $(L/D)_{max}$.

There was considerably less improvement in the lift-drag ratios due to twist and camber at 60° 42' sweep angle than at 50° 38'. It appears that the greatest improvements might be expected at the design sweep angle, although increasing the sweep angle to 60° 42' did not reduce the performance characteristics compared with the flat wing results at 60° 42' sweepback.

[redacted]

Pitching-Moment Characteristics

Comparison of the $\partial C_m/\partial C_L$ curves (fig. 7) shows that, below 0.85 Mach number, twisting and cambering the wing resulted in slightly more forward locations of the aerodynamic center, but above $M = 0.90$, twist and camber resulted in about 1 to 3.5 percent more rearward location of the aerodynamic center. The usual large rearward movement of the aerodynamic center that is expected in the mixed-flow region between $M = 0.90$ and $M = 1.0$ was only partly realized for either wing, although above a Mach number of 1.0 a rather large rearward shift in the aerodynamic-center location was observed for both wings. The experimental results indicated aerodynamic-center locations much farther rearward than those predicted by theoretical calculations (see table I).

The pitching-moment coefficient at zero lift $C_{m_{C_{L=0}}}$ was practically unaffected by twisting and cambering the wing. The 50° 38' swept wing (reference 1) experienced considerably more shift in $C_{m_{C_{L=0}}}$ due to twist and camber. As was pointed out in reference 1, the effect of camber on $C_{m_{C_{L=0}}}$ is opposite to that of twist, and the net effect for a given twisted and cambered wing therefore is the algebraic sum of two separate effects. It appears that for the 60° 42' swept wing these effects are more nearly compensating than for the 50° 38' swept wing.

CONCLUSIONS

An investigation of the effects of twist and camber on the aerodynamic characteristics of a 60° 42' sweptback wing indicated the following conclusions:

1. The twisted and cambered wing gave very little increase in the maximum lift-drag ratios below a Mach number of 0.95 and above a Mach number of 1.05; however, in the Mach number range between 0.95 and 1.05 the twisted and cambered wing produced about 6 to 12 percent higher maximum lift-drag ratios than the untwisted, uncambered wing.

2. The lift, minimum drag, and pitching-moment characteristics were only slightly affected by twisting and cambering the wing.

[redacted]

3. It appears that a twisted and cambered wing designed for 50° sweepback would not incur any losses in performance and stability due to twist and camber when rotated to 60° sweepback.

Langley Aeronautical Laboratory
National Advisory Committee for Aeronautics
Langley Field, Va.

REFERENCES

1. Spreemann, Kenneth P., and Alford, William J., Jr.: Investigation of the Effects of Twist and Camber on the Aerodynamic Characteristics of a 50° 38' Sweptback Wing of Aspect Ratio 2.98. Transonic-Bump Method. NACA RM L51C16, 1951.

2. DeYoung, John, and Harper, Charles W.: Theoretical Symmetric Span Loading at Subsonic Speeds for Wings Having Arbitrary Plan Form. NACA Rep. 921, 1948.

[redacted]

TABLE I

COMPARISON OF PERTINENT EXPERIMENTAL AND THEORETICAL PARAMETERS AT TWO MACH NUMBERS

Parameter	Mach number	Experimental		Theoretical (reference 2)
		Flat wing	Twisted and cambered wing	
$\frac{\partial C_L}{\partial \alpha}$	0.6 .8	0.042 .042	0.041 .041	0.0345 .0335
$y_{c.a.l.}$	0.6 .8	45.8 45.2	46.0 46.0	44.6 44.5
$\frac{\partial C_m}{\partial C_L}$	0.6 .8	-0.095 -.095	-0.090 -.080	-0.004 -.005

[redacted]

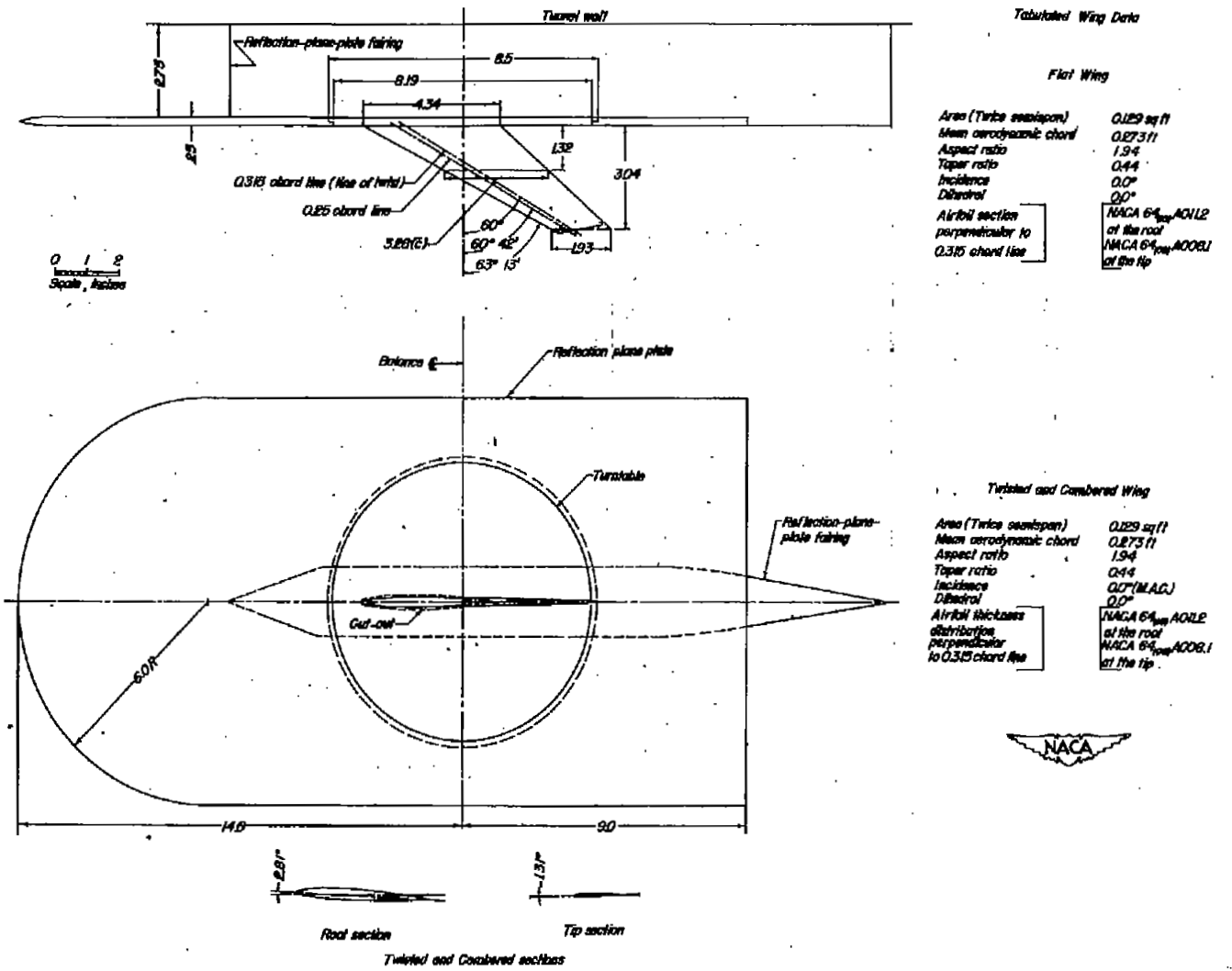

Figure 1.- Test model mounted on the reflection plane in the Langley high-speed 7- by 10-foot tunnel.

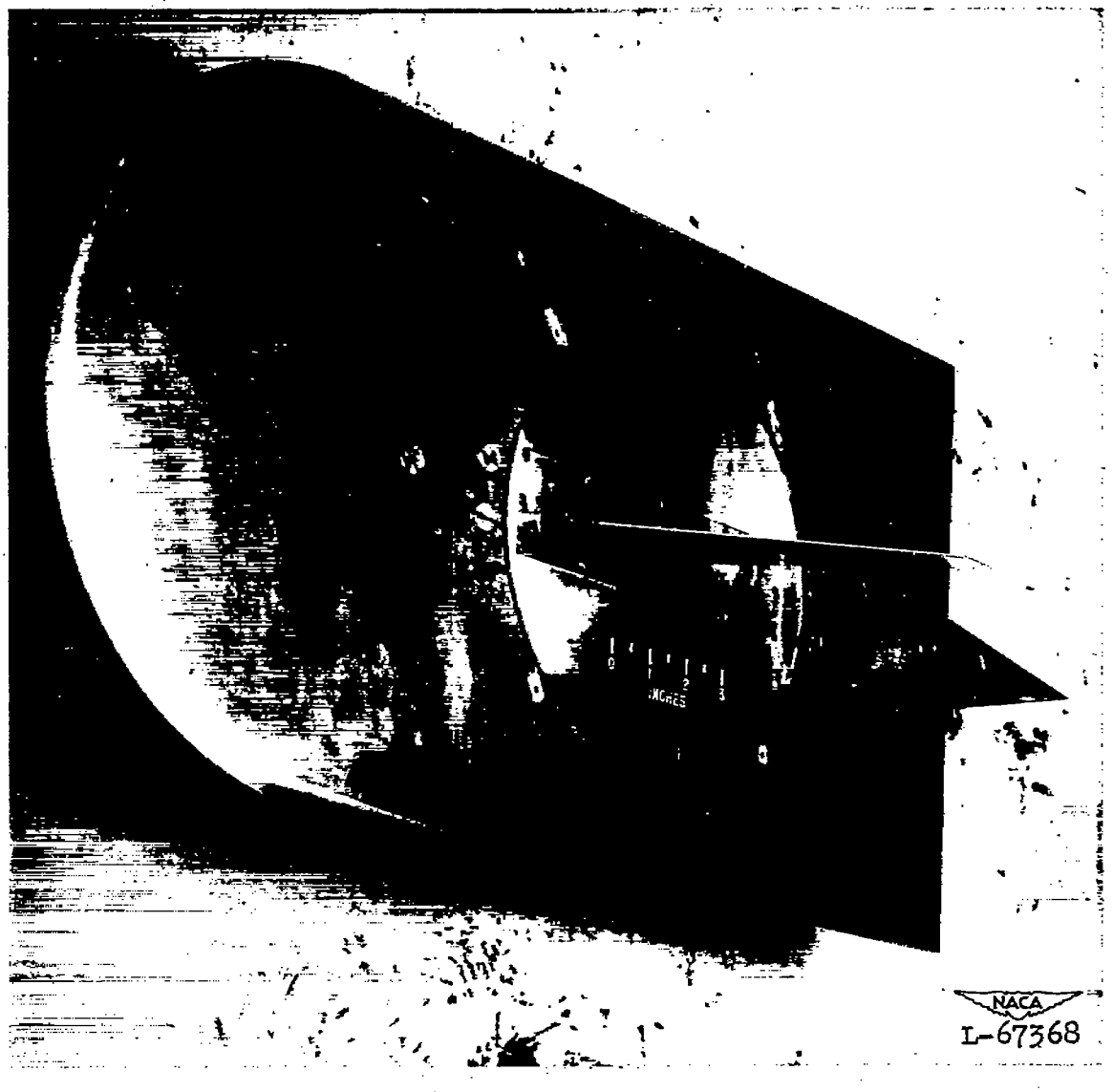

Figure 2.- View of typical test model mounted on the reflection-plane plate in the Langley high-speed 7- by 10-foot tunnel.

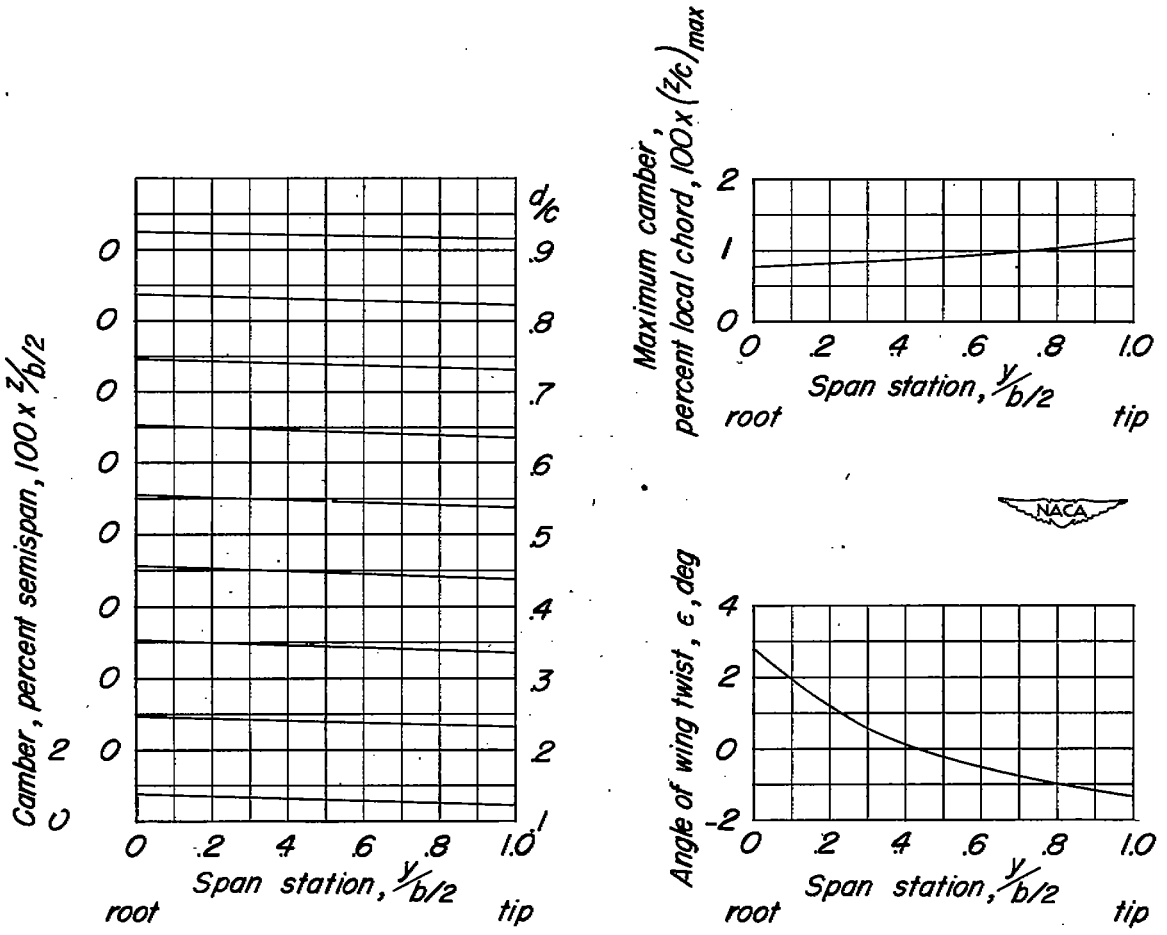

Figure 3.- Spanwise variations of twist and camber of the twisted and cambered wing.

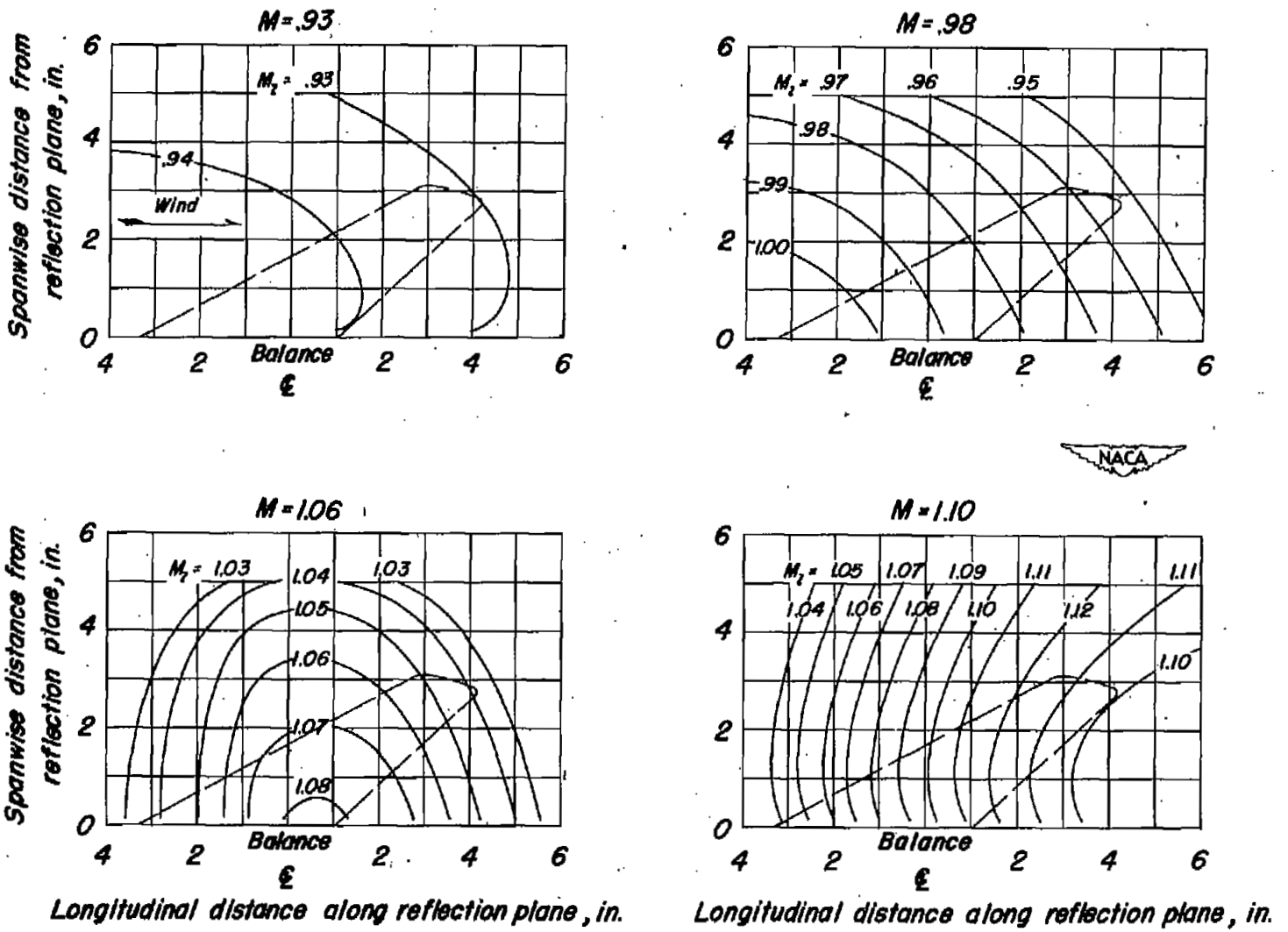

Figure 4.- Typical Mach number contours over sidewall reflection plane in region of model location.

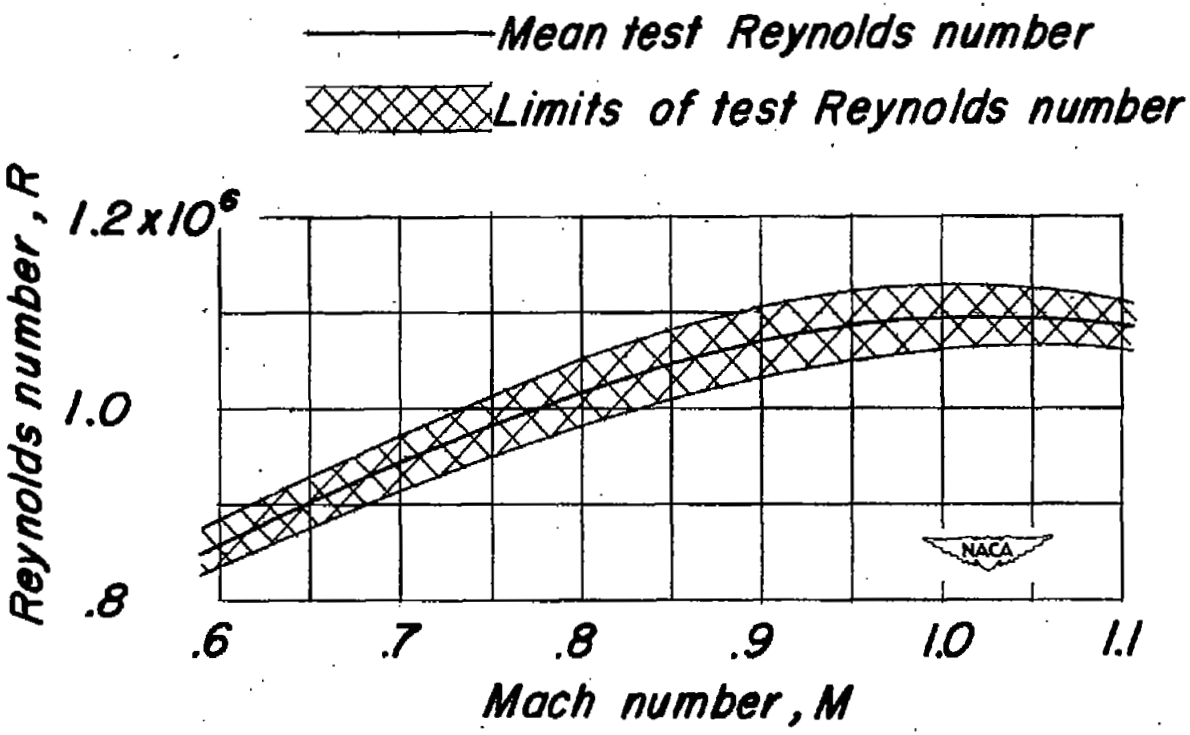

Figure 5.- Variation of test Reynolds number with Mach number for the test models.

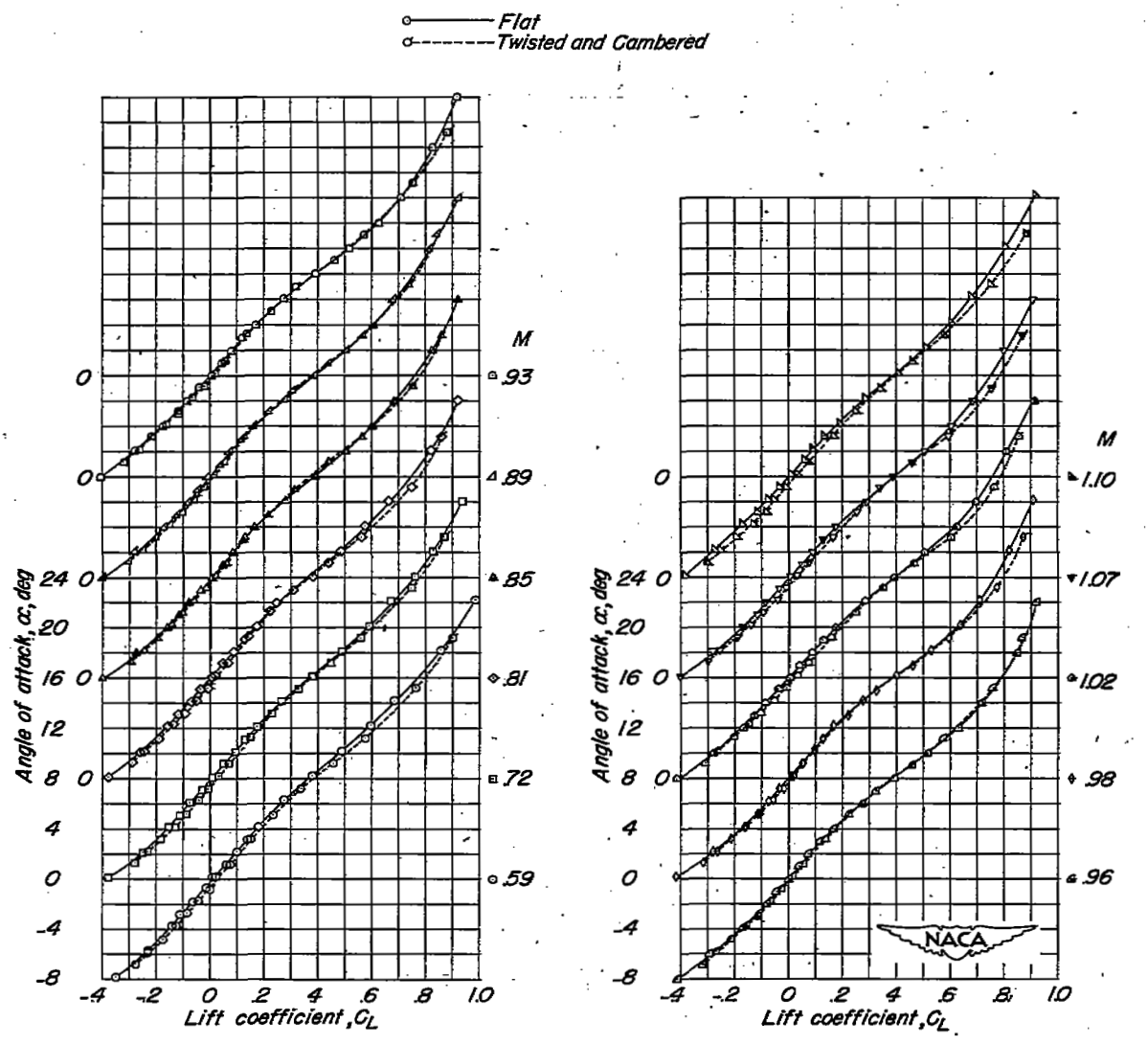

Figure 6.- Aerodynamic characteristics of the test models.

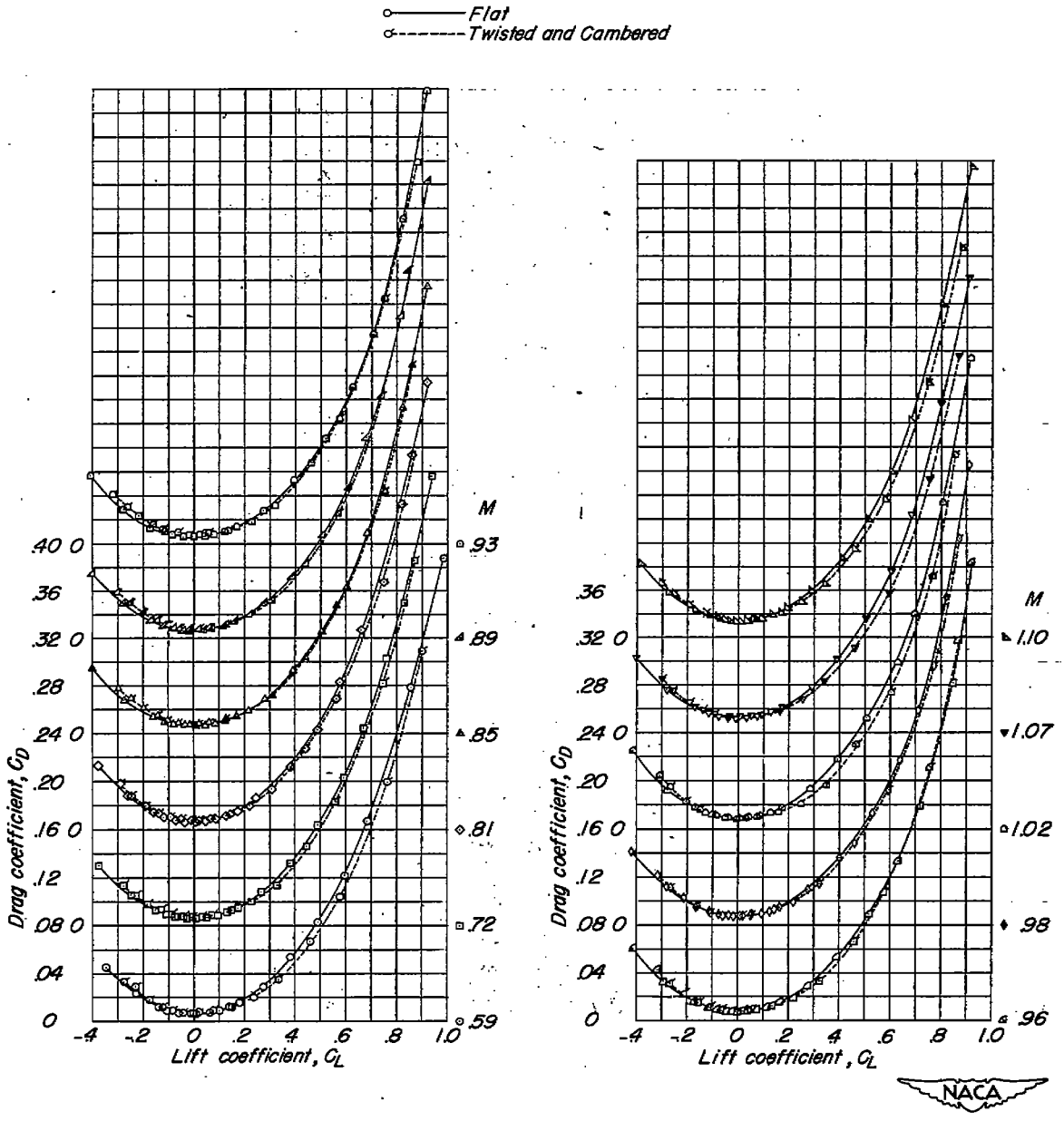

Figure 6.- Continued.

[redacted]

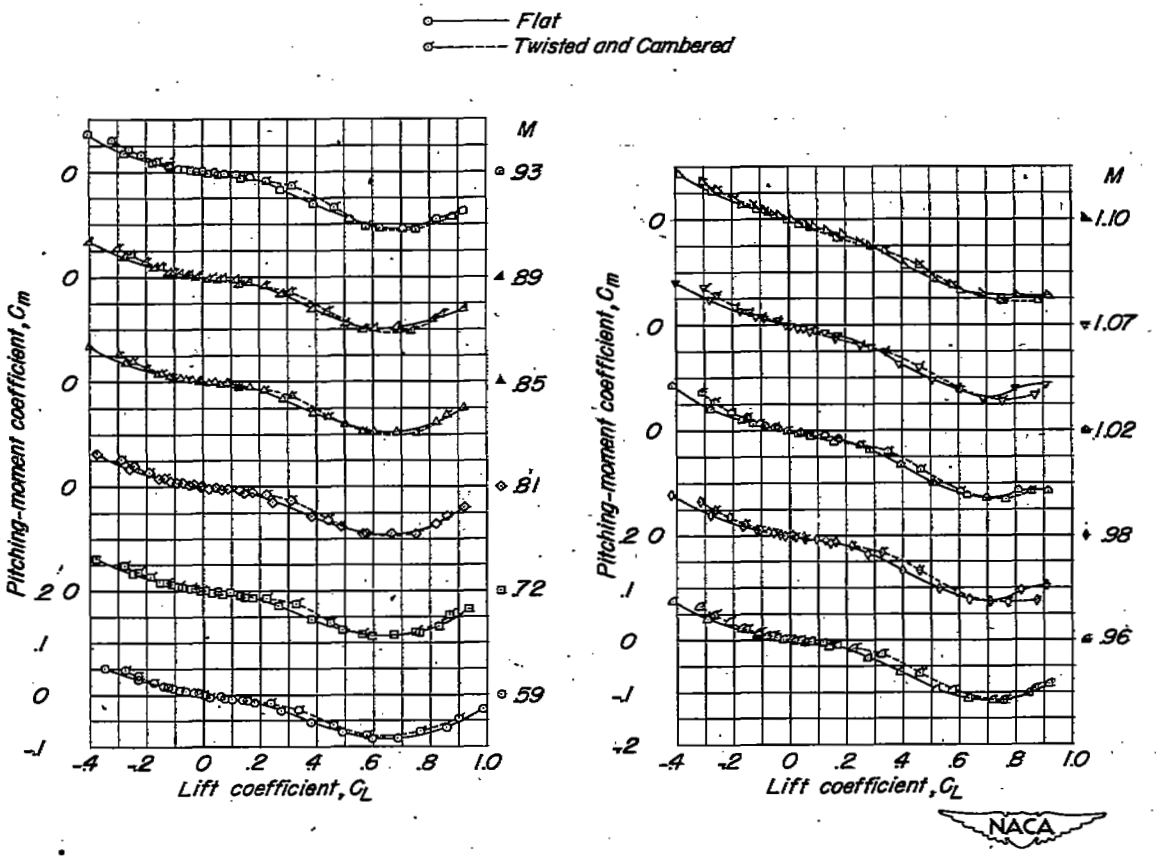

Figure 6.- Continued.

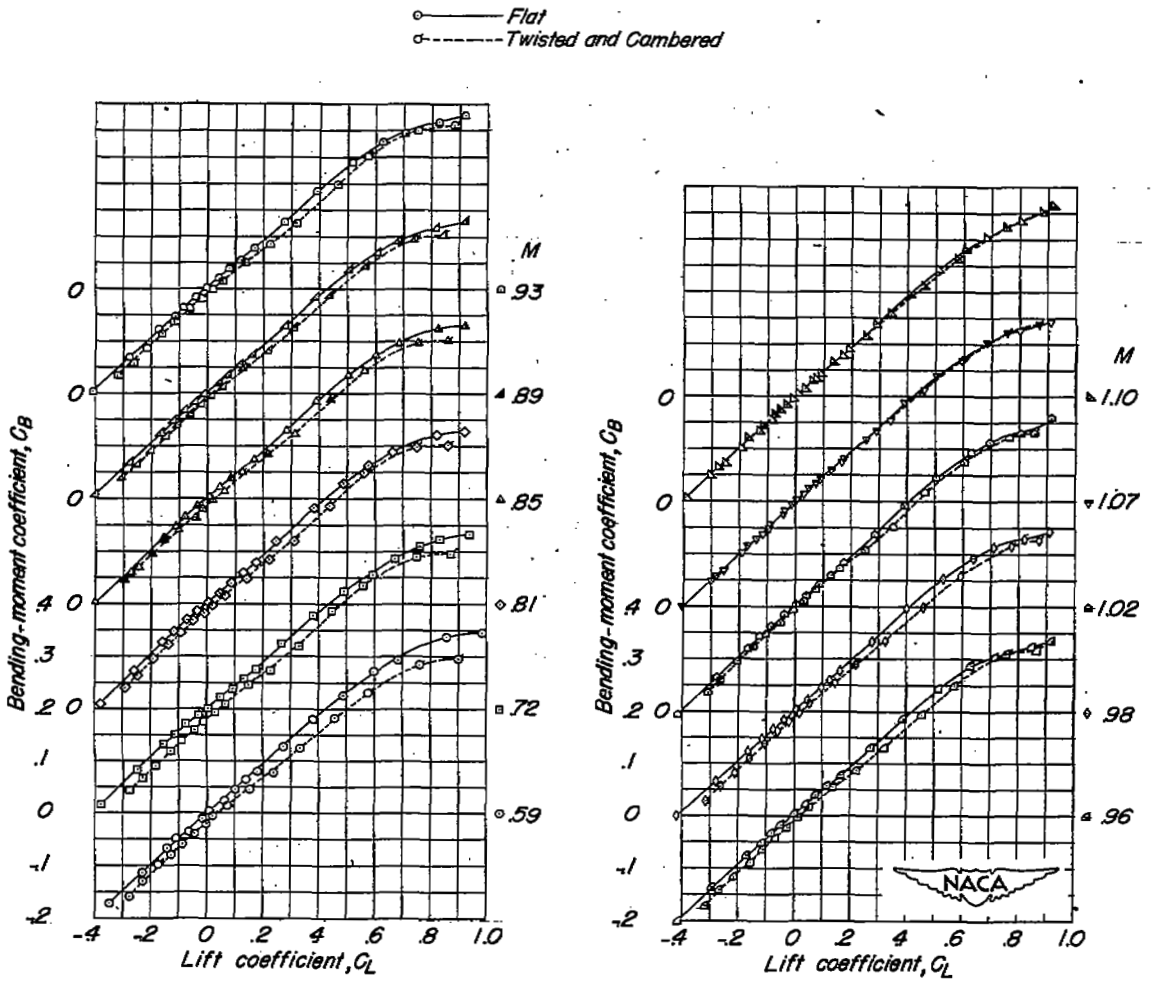

Figure 6.- Concluded.

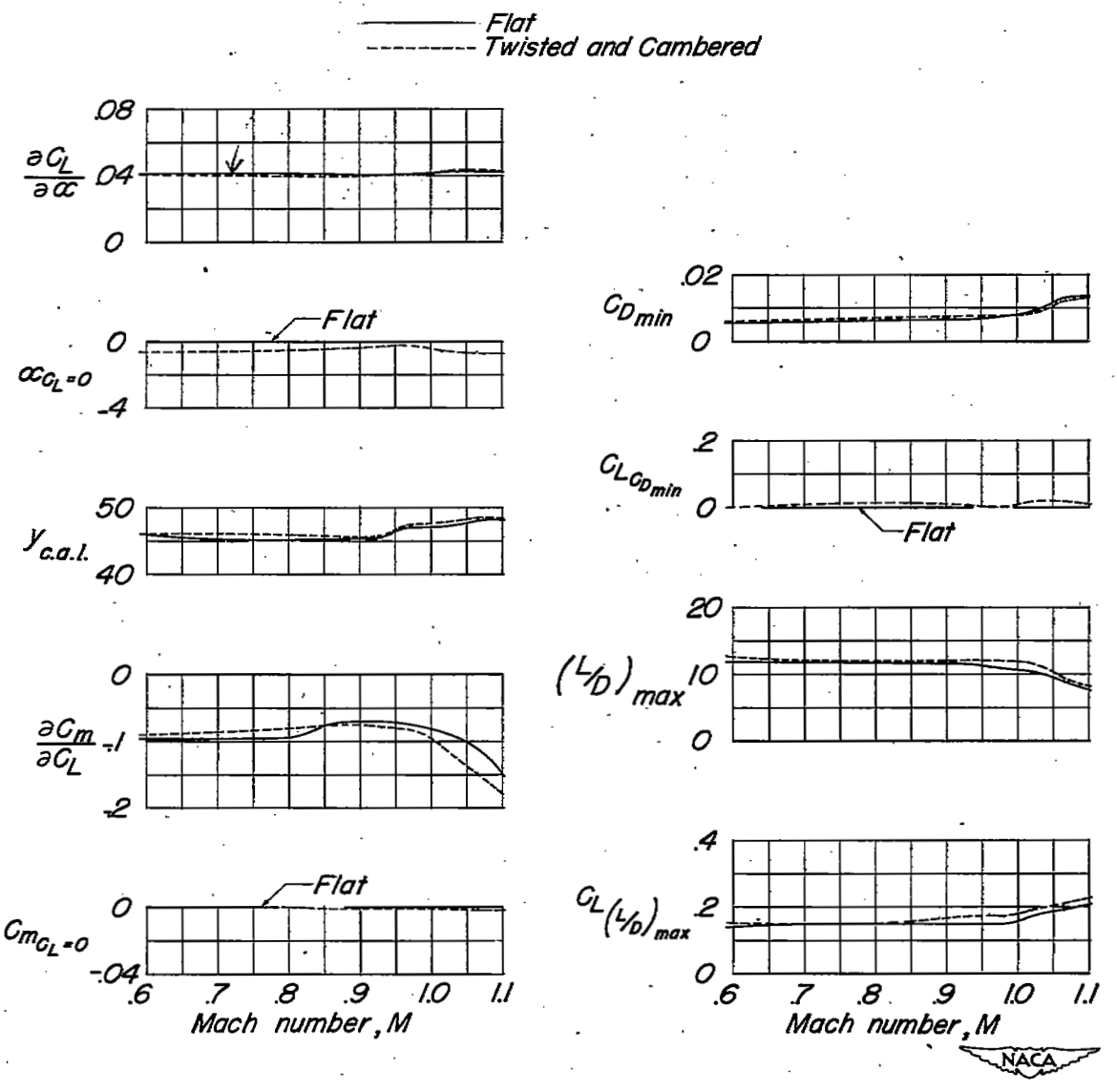

Figure 7.- Summary of the aerodynamic characteristics of the test models. (Slopes are averaged over lift-coefficient range of ±0.1.)

[redacted]